THE ASTROPHYSICAL JOURNAL, 581:L59–L62, 2002 December 10

SPECKLE DECORRELATION AND DYNAMIC RANGE IN SPECKLE NOISE–LIMITED IMAGING

ANAND SIVARAMAKRISHNAN
Space Telescope Science Institute, 3700 San Martin Drive, Baltimore, MD 21218
JAMES P. LLOYD
Department of Astronomy, University of California at Berkeley, 601 Campbell Hall, Berkeley, CA 94720
PHILIP E. HODGE
Space Telescope Science Institute, 3700 San Martin Drive, Baltimore, MD 21218
AND
BRUCE A. MACINTOSH
Institute of Geophysics and Planetary Physics, Lawrence Livermore National Laboratory, University of California, P. O. Box 808, Livermore, CA 94550
Received 2002 September 21; accepted 2002 October 23; published 2002 November 15

ABSTRACT

The useful dynamic range of an image in the diffraction-limited regime is usually limited by speckles caused by residual phase errors in the optical system forming the image. The technique of speckle decorrelation involves introducing many independent realizations of additional phase error into a wave front during one speckle lifetime, changing the instantaneous speckle pattern. A commonly held assumption is that this results in the speckles being "moved around" at the rate at which the additional phase screens are applied. The intention of this exercise is to smooth the speckles out into a more uniform background distribution during their persistence time, thereby enabling companion detection around bright stars to be photon noise limited rather than speckle limited. We demonstrate analytically why this does not occur and confirm this result with numerical simulations. We show that the original speckles must persist and that the technique of speckle decorrelation merely adds more noise to the original speckle noise, thereby degrading the dynamic range of the image.

Subject headings: instrumentation: adaptive optics — methods: analytical — methods: numerical — space vehicles: instruments — techniques: image processing

1. INTRODUCTION

The recent indirect detection of extrasolar planets has fueled extensive interest in the prospects for direct detection of light from an extrasolar planet with either ground-based adaptive optics (AO) or a space coronagraph. Even moderate sized telescopes achieve sufficient resolution to spatially resolve the planet from the parent star. However, the challenge is achieving sufficient contrast to discriminate the light from the planet against the residual background light from the star. To the extent this background is stable, it can be subtracted. However, the subtraction of the point-spread function (PSF) is typically limited by temporally variable PSF fluctuations (speckles), which are not stable enough to be subtracted yet not variable enough to average out to the required level.

Ground-based AO systems correct incoming stellar wave fronts in real time to create a diffraction-limited image. Based on photon statistics for an AO-corrected image, Nakajima (1994) concluded that direct detection of extrasolar planets was feasible, even with 4 m class ground-based telescopes. However, the well-corrected AO image is composed of a diffraction-limited, bright core accompanied by speckles of light that are the result of imperfect correction by the AO system. It is the existence and relative longevity of these residual speckles that limit the dynamic range of long-exposure images, not photon noise (Racine et al. 1999). Space telescopes suffer from similar effects, variable speckles resulting from midfrequency mirror polishing errors, modulated by internal spacecraft motions and vibrations.

The fundamental idea of speckle decorrelation (also known as "phase boiling" or "hyperturbulation;" Saha 2002) is to scramble the bright residual speckles of the image into a smooth background on a faster timescale than the speckle dwell time, thereby reducing the local spatial variance of the intensity distribution of the PSF, in order to increase our ability to detect a faint companion or faint structure near the star (Angel 1994). This additional phase noise either can be deliberately introduced or is simply the result of wave front sensing noise in an AO system. This concept, although widely cited (Saha 2002; Canales & Cagigal 2000; Boccaletti, Moutou, & Abe 2000; Racine et al. 1999; Woolf & Angel 1998; Angel & Burrows 1995; Stahl & Sandler 1995), has not been demonstrated to exist. Stahl & Sandler (1995) attempted to address this problem with simulations, but these simulations were primarily directed toward simulating the AO system and do not prove or disprove the existence of speckle decorrelation. The effect of boiling phases has also been investigated in the context of the dark speckle method (Labeyrie 1995; Aime 2000), with the conclusion that appropriate phase boiling can improve the signal-to-noise ratio. However, dark speckle methods are fundamentally different from direct imaging in that they select preferred components of the PSF fluctuations, and dark speckle conclusions do not apply to long-exposure images.

2. SECOND-ORDER EXPANSION OF THE PSF

The telescope entrance aperture and all phase effects in a monochromatic wave front impinging on the optical system can be described by a real aperture illumination function $A(x, y)$ multiplied by a unit modulus function $e^{i\phi(x, y)}$. Aperture plane coordinates are (x, y) in units of the wavelength of the light, and image plane coordinates are (ξ, η) in radians. Here phase variations induced by the atmosphere or imperfect optics are described by a real wave front phase function ϕ. We neglect the effects of scintillation. We can force ϕ to possess a zero mean value over the entire aperture plane without any loss of generality,

so

$$\int A\phi \, dx \, dy \Big/ \int A \, dx \, dx = 0. \quad (1)$$

Although it is not a requirement imposed by the mathematics, it is most convenient to locate the image plane origin at the centroid of the image PSF, which corresponds to a zero mean tilt of the wave front over the aperture.

At any location in the pupil plane, the function $e^{i\phi(x,y)}$ can be expanded in an absolutely convergent series for any finite values of the phase function:

$$e^{i\phi(x,y)} = 1 + i\phi - \phi^2/2 + \ldots . \quad (2)$$

The electric field strength in the image plane, $E(\xi, \eta)$, is the Fourier transform of $Ae^{i\phi(x,y)}$. Truncating the above expansion above the second order in ϕ, we calculate the PSF of the image to be

$$\begin{aligned} p(\Phi) = {} & aa^* \\ & - i[a(a^* \star \Phi^*) - a^*(a \star \Phi)] \\ & + (a \star \Phi)(a^* \star \Phi^*) \\ & - \tfrac{1}{2}[a(a^* \star \Phi^* \star \Phi^*) + a^*(a \star \Phi \star \Phi)], \end{aligned} \quad (3)$$

where a is the Fourier transform of the real aperture illumination function A, Φ is the Fourier transform of the AO-corrected wave front phase error ϕ, the star symbol denotes the convolution operator, and the asterisk indicates complex conjugation. This truncated expansion for the PSF is valid when the aberration at any point in the pupil is significantly less than a radian.

The first term in the expansion in equation (3) is the perfectly corrected PSF $p_0 = aa^*$, which is symmetric, regardless of aperture geometry or apodization.

The second term,

$$p_1(\Phi) = -i[a(a^* \star \Phi^*) - a^*(a \star \Phi)] = 2 \, \mathrm{Im}\,[a(a^* \star \Phi^*)], \quad (4)$$

is a real, antisymmetric perturbation of the perfect PSF. It is modulated in size by the amplitude-spread function (ASF) a: any bright first-order speckle due to this term is "pinned" to the bright rings of the perfect ASF (Bloemhof et al. 2001). However, because $a(a^* \star \Phi^*)$ is Hermitian, such speckles must be accompanied by a corresponding dimming of the PSF at a diametrically opposed point in the image. This result is also independent of aperture geometry, although pupil apodization will affect the underlying ring structure of a.

The third term,

$$p_{2,\,\mathrm{halo}}(\Phi) = (a \star \Phi)(a^* \star \Phi^*), \quad (5)$$

is real and nonnegative everywhere, zero at the image center (because of our choice of the phase zero point as described by eq. [1]), and symmetric about the center. It is the power spectrum of the real function $A\phi$. This term places speckles in the dark areas of a monochromatic PSF and therefore sets the ultimate limits on the dynamic range of any observational "speckle sweeping" techniques described in Bloemhof et al. (2001).

The last term,

$$p_{2,\,\mathrm{Strehl}}(\Phi) = -\tfrac{1}{2}[a(a^* \star \Phi^* \star \Phi^*) + a^*(a \star \Phi \star \Phi)], \quad (6)$$

is also modulated by the size of the ASF a, just like the first-order term, $p_1(\Phi)$. At the origin, it reduces to the extended Maréchal approximation relating the Strehl ratio S to the variance of the phase over the aperture, σ_ϕ^2, at high Strehl ratios: $S \simeq 1 - \sigma_\phi^2$.

We analyze the statistics of speckle contamination of images using this second-order expansion for the PSF of a well-corrected image.

3. THE SPECKLE DECORRELATION MODEL

The speckle decorrelation technique can be modeled by adding N uncorrelated, independent realizations of phase noise $\psi_k(x)$ to the wave front (with a deformable mirror, for example) while the exposure is in progress. The index k runs from 1 through N. We assume that the N artificial phase error realizations are asserted for equal time intervals, $\tau = T/N$, during a speckle lifetime T. Each of the ψ_k's is constructed to possess a zero aperture-weighted mean as well as the same mean tilt across the aperture as ϕ.

The PSF of the exposure that lasts the length of the speckle lifetime T will therefore be the average of individual PSFs p_k, each of which is formed by a wave front with a phase of $(\phi + \psi_k)$. The PSF during the time the kth phase screen is added to the residual phase ϕ is

$$p_k = p(\Phi + \Psi_k), \quad (7)$$

where Ψ_k is the Fourier transform of ψ_k (using eq. [3]). The PSF of an image with exposure time T is the average of each of the individual PSFs:

$$\bar{p} = \Sigma_k p_k / N. \quad (8)$$

Since a and Φ are constant for the duration of the exposure, the summation in equation (8) can be moved to within the multiplications and convolution integrals in equations (7) and (3).

If we expand p_k in the manner of equation (3), we obtain

$$\begin{aligned} p_{0,\,k} &= p_0(\Phi), \\ p_{1,\,k} &= p_1(\Phi) + p_1(\Psi_k), \\ p_{2,\,\mathrm{halo},\,k} &= p_{2,\,\mathrm{halo}}(\Phi) + p_{2,\,\mathrm{halo}}(\Psi_k) \\ &\quad + (a \star \Phi)(a^* \star \Psi_k^*) + (a^* \star \Phi^*)(a \star \Psi_k), \\ p_{2,\,\mathrm{Strehl},\,k} &= p_{2,\,\mathrm{Strehl}}(\Phi) + p_{2,\,\mathrm{Strehl}}(\Psi_k) \\ &\quad - [a(a^* \star \Phi^* \star \Psi_k^*) + a^*(a \star \Phi \star \Psi_k)]. \end{aligned}$$

Averaging each of these terms over the N realizations of ψ_k, with their corresponding transforms Ψ_k, produces average in-

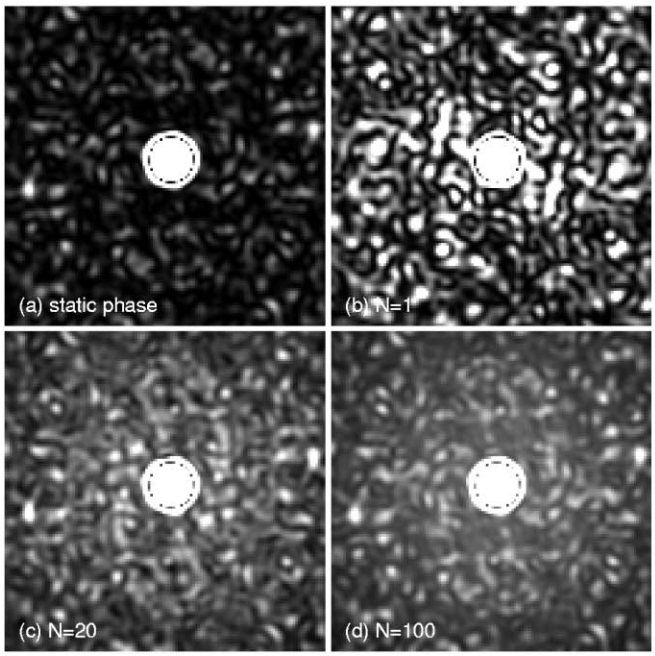

FIG. 1.—(*a*) Simulated (e.g., AO-corrected) PSF with a residual fitting error of 17 nm rms, producing a speckle pattern. (*b*) PSF of a 20 nm rms independent phase error added to that used in (*a*). (*c*) Sum of 20 PSFs, each with the same residual error as (*a*) and independent 20 nm phase errors as in (*b*). (*d*) Sum of 100 PSFs as in (*c*) (see text for details).

tensities of

$$\bar{p_0} = p_0(\Phi),$$

$$\bar{p_1} = p_1(\Phi) + \Sigma_k p_1(\Psi_k)/N,$$

$$\bar{p}_{2,\,\mathrm{halo}} = p_{2,\,\mathrm{halo}}(\Phi) + \Sigma_k p_{2,\,\mathrm{halo}}(\Psi_k)/N + (a \star \Phi)(a^* \star \Sigma_k \Psi_k^*)/N + (a^* \star \Phi^*)(a \star \Sigma_k \Psi_k)/N,$$

$$\bar{p}_{2,\,\mathrm{Strehl}} = p_{2,\,\mathrm{Strehl}}(\Phi) + \Sigma_k p_{2,\,\mathrm{Strehl}}(\Psi_k)/N - [a(a^* \star \Phi^* \star \Sigma_k \Psi_k^*) + a^*(a \star \Phi \star \Sigma_k \Psi_k)]/N,$$

in the final image. The sum of these individual averages is the final PSF of the image. The quantity $S_k(\xi, \eta) = \Sigma_k \Psi_k$ or its conjugate appear frequently in the averaged PSF; S_k is zero mean, with a standard deviation of $\sigma_\Psi/\sqrt{N}$ (where $\sigma_\Psi^2(\xi, \eta)$ is the variance of the parent distribution of the random phase functions' Fourier transforms).

The zeroth-order term remains aa^*. The first-order contribution of the N "speckle decorrelating" phase screens to $\bar{p}$ is $\Sigma_k p_1(\Psi_k)/N$, which is a zero mean quantity. It can be rewritten as 2 Im $[a(a \star S_k)]$.

The $\bar{p}_{2,\,\mathrm{halo}}$ term is composed of the sum of the original halo term and the expectation value of the halo term calculated over the ensemble of phase error functions, because both $(a \star \Phi)(a^* \star S_k^*)/N$ and $(a^* \star \Phi^*)(a \star S_k)/N$ have zero expectation values.

Likewise, the $\bar{p}_{2,\,\mathrm{Strehl}}$ term is composed of the sum of the original Strehl term and the expectation value of the individual Strehl term calculated over the ensemble of the phase error functions, because $a(a^* \star \Phi^* \star S_k^*)$ and $a^*(a \star \Phi \star S_k)$ have zero expectation values.

None of the zero mean terms contribute in a manner that will alter the long-exposure image in the limit as N becomes large. Therefore, the resulting image formed by the addition of small (in the perturbation theory sense) phase noise does not result in speckle decorrelation.

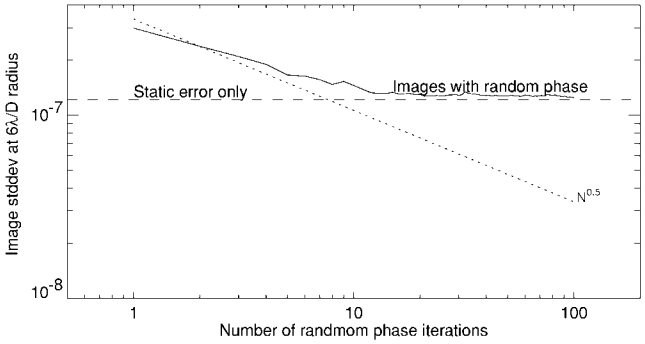

FIG. 2.—Image noise (measured as the standard deviation of the intensity values in an annulus) as a function of the number of separate images added together. The noise eventually reaches a plateau equal to the noise in an image having only the original residual phase error (see text for details).

4. NUMERICAL SIMULATIONS

We have carried out numerical simulations to illustrate this point. Figure 1*a* shows a simulated image created from a small static phase error with an rms magnitude of 17 nm at a wavelength of 1.6 μm. (In this case, the image simulated the residual atmospheric fitting error in an AO correction, but we could have used any error with an approximately flat power spectrum over the region of the image.) Diffraction rings have been suppressed at radii greater than 0.″1 by using pupil apodization. We then simulated a random phase error by injecting 20 nm of white phase noise into the phase residuals. These were convolved with a Gaussian kernel to represent the same actuator spacing as was used to generate the fitting error (following the method outlined in Sivaramakrishnan et al. 2001), but this could represent any error with a similar power spectrum to the static error. Figure 1*b* shows the resultant image, showing an entirely new speckle pattern. We simulated the long-exposure image process by keeping the static error fixed, injecting different realizations of the white noise, and adding together the resultant images, thereby attempting to smooth out a long-lived speckle pattern with a very fast moving speckle pattern. Figure 1*c* shows the result after 20 iterations, and Figure 1*d* after 100 iterations; the image speckle pattern has returned to the original pattern, offset by a pedestal equal to the average intensity of the random speckle pattern.

Figure 2 shows this quantitatively. This is a plot of the image noise (measured as the standard deviation of the intensity values in an annulus) as a function of the number of separate images added together. The noise initially declines rapidly as the speckles due to the white noise average together, but ultimately the noise reaches a plateau equal to the noise in an image having only the original fitting error common to all the images.

On the face of it, this appears to contradict the simulations of Stahl & Sandler (1995). However, the results are actually consistent with their work. Their initial simulations showed a

long-lived speckle pattern that changed only on atmospheric timescales, which they attributed to a large wave front error caused by time lags. (It may have been augmented by the lack of a wave front reconstructor algorithm—instead, direct average phase measurements were applied directly to their simulated dispersion measure.) When they changed their AO model to incorporate a predictive controller with lower time lags, the speckle pattern began to change rapidly. The effect of the predictive controller, however, is not to decorrelate the speckles due to atmospheric time lag but to reduce the residual wave front error due to this source and hence the total intensity of the long-lived speckle pattern; this left the short-lived speckles due to measurement error as the main remaining noise source. Stahl & Sandler did not demonstrate speckle decorrelation but speckle suppression. One can always reduce speckle noise by reducing the corresponding wave front error term; what one cannot do is change the timescale of a given speckle error term by introducing other zero mean phase errors uncorrelated with the phase errors causing the original speckle. (In addition, the short timescales simulated by Stahl & Sandler may have masked longer lived speckle effects, and the coarse sampling of their simulations may also have masked the real evolution of noise sources.)

5. ALTERNATIVES TO SPECKLE DECORRELATION

Each term in the series expansion of the PSF possesses distinct properties. Further work on characterizing the magnitude of the various terms (in both monochromatic and polychromatic cases), assuming either AO-corrected atmospheric turbulence or typical mirror aberrations, is being done in order to assess how one might use the knowledge of these properties to improve dynamic range. The first-order term has already been treated in the literature (Bloemhof et al. 2001; Boccaletti, Riaud, & Rouan 2002), although the second-degree term $p_{2,\,\mathrm{Strehl}}$ is often the largest term close to the image core. Furthermore, when using speckle sweeping techniques, it is likely that ultimate dynamic range limits in the wings of the PSF are set by the other second-degree term, $p_{2,\,\mathrm{halo}}$.

The authors wish to thank the Space Telescope Science Institute's Research Programs Office and its Director's Discretionary Research Fund. This work has also been supported by the National Science Foundation Science and Technology Center for Adaptive Optics, managed by the University of California at Santa Cruz under cooperative agreement AST 98-76783, the Australian Fulbright Commission, and the SPIE Irving J. Spiro fellowship. Portions of this work were performed under the auspices of the US Department of Energy, National Nuclear Security Administration, by the University of California, Lawrence Livermore National Laboratory, under contract W-7405-Eng-48.

REFERENCES

Aime, C. 2000, J. Opt. A, 2, 411
Angel, J. R. P. 1994, Nature, 368, 203
Angel, R., & Burrows, A. 1995, Nature, 374, 678
Bloemhof, E. E., Dekany, R. G., Troy, M., & Oppenheimer, B. R. 2001, ApJ, 558, L71
Boccaletti, A., Moutou, C., & Abe, L. 2000, A&AS, 141, 157
Boccaletti, A., Riaud, P., & Rouan, D. 2002, PASP, 114, 132
Canales, V. F., & Cagigal, M. P. 2000, A&AS, 145, 445
Labeyrie, A. 1995, A&A, 298, 544
Nakajima, T. 1994, ApJ, 425, 348
Racine, R., Walker, G. A. H., Nadeau, D., Doyon, R., & Marois, C. 1999, PASP, 111, 587
Saha, S. K. 2002, Rev. Mod. Phys., 74, 551
Sivaramakrishnan, A., Koresko, C. D., Makidon, R. B., Berkefeld, T., & Kuchner, M. J. 2001, ApJ, 552, 397
Stahl, S. M., & Sandler, D. G. 1995, ApJ, 454, L153
Woolf, N., & Angel, J. R. 1998, ARA&A, 36, 507